Chemical Physics 488–489 (2017) 36–42

Contents lists available at ScienceDirect

Chemical Physics

journal homepage: www.elsevier.com/locate/chemphys

Theoretical study of electronic properties and isotope effects in the UV absorption spectrum of disulfur ☆

Karolis Sarka [a], Sebastian O. Danielache [a], Alexey Kondorskiy [b], Shinkoh Nanbu [a,*]

[a] Department of Materials and Life Sciences, Faculty of Science and Technology, Sophia University, 7-1 Kioi-Cho, Chiyoda-ku, Tokyo 102-8554, Japan
[b] P.N. Lebedev Physical Institute of the Russian Academy of Sciences, 53 Leninskiy pr., Moscow 119991, Russia

ARTICLE INFO

Article history:
Received 8 February 2017
In final form 15 March 2017
Available online 22 March 2017

Keywords:
Potential energy curves
Absorption cross-section
Photodissociation
Isotope effects

ABSTRACT

The electronic structures of triplet S_2 ground and excited states are studied by *ab initio* molecular orbital and configuration interaction calculation. Potential energy curves correlated with $S(^3P) + S(^3P)$ and $S(^3P) + S(^1D)$ at the dissociation limit are evaluated, and electronic terms for a total of 11 states are assigned. Transition dipole moments, as a function of internuclear distance, are determined for two allowed transitions to $1^3\Pi_u$ and $1^3\Sigma_u^-$ excited states. Furthermore, the total absorption cross-sections are computed to estimate isotope-fractionation constants, ε, for four most common isotopologues: $^{32}S^{32}S$, $^{32}S^{33}S$, $^{32}S^{34}S$, and $^{32}S^{36}S$ by quantum close-coupling (R-matrix) expansion approach. Zero-point energy based constants ε^{ZPE} are estimated as well to compare with the obtained isotope effects. Three-isotope plots are shown to express mass-independent fractionation effect; large isotopic effects were found on ^{36}S and ^{33}S in 230–240 nm range, and only on ^{36}S in 240–267 nm range.

1. Introduction

Most sulfur trace molecules have a strong absorption in 180–300 nm range [1–4], which means, that in the present atmosphere, most tropospheric sulfur-containing molecules are shielded from UV radiation by the ozone layer, and undergo oxidation to sulfuric acid and formation of sulfate particles. The photochemistry introducing mass-independent isotopic fractionation (MIF) effects is limited to high altitudes and the isotopic ratio of washed out sulfates has a close resemblance to the emitting source. However, before the oxygen levels rose and stabilized in the atmosphere, approximately 2.5 Ga ago, a large fluctuation in sulfur isotope abundance was observed. During the Archean period the lack of oxygen in atmosphere created a significant increase in actinic flux of shorter wavelengths [5], leading to a large increase in photochemical activity of atmospheric sulfur. The major sources of sulfur-containing molecules were volcanic eruptions and outgassing, and marine outgassing; mostly in a form of SO_2 and H_2S [6–9]. Due to the increased solar flux in mid-UV range in anoxic atmosphere, sulfur compounds undergo several reducing photodissociation steps: sulfur dioxide is photolyzed to SO + O which undergoes photolysis again to produce S + O; skewing the ratio of isotopologues due to MIF [2,4,10,11]. Sulfur atoms recombine with each other and form S_2 molecule [12]. The photochemical cycle of $S_2 \leftrightarrow S_8$ was a crucial part of the general photochemistry: a source of elemental sulfur particles in the atmosphere. A large positive $\Delta^{33}S$ was observed in elemental sulfur deposits, which were formed largely by particle precipitation and deposition of S_8-based particles in Archean period [7]. A large MIF effect is suspected in the photolysis of S_2 and S_4.

The sulfur photochemistry in 0th oxidation state needs an atmosphere that meets three requirements: low levels of atmospheric O_2, a source of H_2S or SO_2, and an abundance of a reduced gas, mostly methane [13]. Judging from the reported vertical distribution of trace gases in an Archean atmosphere, we can see that the levels of CH_4 high enough to sustain $S_2 \leftrightarrow S_8$ cycle and prevent oxidation, were met up to 50 km altitude [14]. Pavlov *et. al.* has modeled the greenhouse effect on Archean atmosphere based on concentration of trace gases, which shows a large variation of temperature based on altitude and reduced trace gas concentration [15]. It is important to study the MIF dependency on temperature, which might relate to the vertical mixing ratio of S_2 and the isotopic enrichment of the elemental sulfur particles. It is suspected, that the following photochemical reaction cycle [12] was a source to the observed isotope abundance variation in geological records: [6]

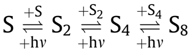

$$S \underset{+h\nu}{\overset{+S}{\rightleftharpoons}} S_2 \underset{+h\nu}{\overset{+S_2}{\rightleftharpoons}} S_4 \underset{+h\nu}{\overset{+S_4}{\rightleftharpoons}} S_8$$

☆ Electronic Supplementary Information (ESI) available online.

* Corresponding author.
E-mail address: shinkoh.nanbu@sophia.ac.jp (S. Nanbu).

http://dx.doi.org/10.1016/j.chemphys.2017.03.005
0301-0104/

The resulting S_8 formed elemental sulfur particles and was washed out of the atmosphere. During these cyclic reactions, any mass-independent isotopic fractionation in the photodissociation process results in a particle with a largely variable sulfur isotope ratio.

Several experimental studies were done in the mid-20th century focusing on electronic structure and assignment of excited states [16–19], as well as rotational properties of S_2 [20], but none of them had produced a study of isotopic effects or the absorption cross-section spectrum.

In the present work, potential energy curves (PECs) and transition dipole moments (TDMs) are computed at a quite fine grid to produce high resolution spectra on isotope-specific photoabsorption cross-sections, wavelength dependent isotope fragmentation factors (ε) and evaluate the MIF; theoretical excitation energies and equilibrium bond distances agree well with the available experimental data. Furthermore, our results clarify that there are large absorption cross-sections in 200–270 nm range with a peak at 254 nm, featuring a continuum band, a vibronic progression band, and a resonance band formed due to the interference between the former two bands. Finally, the isotopic fractionation constant, ε, has been computed for three isotopologues ($^{32}S^{33}S$, $^{32}S^{34}S$ and $^{32}S^{36}S$) assuming that the cross-section would be proportional to photolysis rate in comparison to the ε based on zero-point energy (ZPE) shift model, introduced by Yung and Miller [21]. Our data suggests much stronger mass-independent isotopic fractionation effect than the ZPE model; the large MIF appears in resonance and progression bands, resulting in depletion of both, ^{33}S and ^{36}S isotopes.

The purpose of this work is to display theoretical data based on modern theory, that might assist further experimental analysis, providing an accurate picture of the electronic states and the absorption cross-section of S_2. In addition to that, we present the basis for further geochemical analysis of this system with respect to mass-independent isotopic fractionation between different isotopologues.

2. Methodology

2.1. Computational details

The potential energy curves were computed using MOLPRO2012 [22] and MRCI-F12 [23] method with aug-cc-pVQZ (augmented, correlation consistent, polarized valence, quadruple-ζ) basis set. The initial orbital guess was obtained at complete active space (CAS) SCF [24]/aug-cc-pVDZ level, which was used to be improved with CASSCF/aug-cc-pVQZ before proceeding to the MRCI-F12 calculations. The transition dipole moments were computed at MRCI [25]/aug-cc-pVQZ level.

To ensure the smoothness of the curves, and to evaluate the exact position of any avoided curve-crossing points, the grid spacing was chosen as follows: 1.7–3.5 Å: 0.01 Å; 3.5–4.5 Å: 0.05 Å; 4.5–5.0 Å: 0.1 Å. At each grid point, energy and electronic configuration of each excited state, together with the transition dipole moment, were estimated, resulting in two states with an allowed dipole transition from the ground electronic state: $1^3\Pi_u$, and $1^3\Sigma_u^-$. Finally, the recently developed version of the R-matrix technique [2] was employed to obtain the UV spectra using the potential energies and transition dipole moments. The essential feature of our technique is the incorporation of the specific accurate and numerically stable algorithm to compute the parameters of the discrete and quasi-discrete states in the systems of nonadiabatically coupled potentials. Using Boltzmann distribution of rotational and vibrational states, absorption cross-sections were computed for four isotopologues: $^{32}S^{i}S$, where $i \in \{32, 33, 34, 36\}$. For each isotopologue we have used $v = 0$ and $J = 0 \ldots 30$ at $T = 100$ K, and $v = 0, 1$ and $J = 0 \ldots 61$ at $T = 298$ K. The isotopologue notation in further text will be denoted as $^{2i}S_2$, where $i \in \{2, 3, 4, 6\}$ for atomic mass of 32, 33, 34 and 36, respectively. Peak broadening was calculated by combination of thermal broadening at 100 K and 298 K, and a natural lifetime, where radiative lifetime of $\tau = 16.9$ ns [26] was used, resulting in FWHH broadening of 0.0316–0.0307 cm^{-1} at 100 K and 0.0531–0.0516 cm^{-1} at 298 K for $^{22}S_2$–$^{26}S_2$ isotopologues.

3. Results and discussion

3.1. Potential energy curves

The electronic terms were assigned following the Wigner-Witmer symmetry rules [27,28]. The dissociation to the $S(^3P) + S(^3P)$ is a collection of six triplet states. Three non-degenerate Σ states: $1^3\Sigma_u^+, 2^3\Sigma_u^+$, and $1^3\Sigma_g^-$; and three double-degenerate states: $1^3\Pi_g, 1^3\Pi_u$, and $1^3\Delta_u$. Three selection rules apply to this system. First, since all electronic states have the angular momentum quantum number Λ, the transitions are only allowed with the following constraint:

$$\Delta\Lambda = 0, \pm 1$$

Since the ground state of S_2 is $1^3\Sigma_g^-$ with quantum number $\Lambda = 0$, the transition to $1^3\Delta_u$ state, with $\Lambda = 2$, is forbidden. The second selection rule is the parity selection rule, which states that *even parity electronic states combine only with odd parity states* ($u \leftrightarrow g, g \not\leftrightarrow g, u \not\leftrightarrow u$), we can rule out the transition to $1^3\Pi_g$ state. The third selection rule applies to the states with same angular momentum, $\Delta\Lambda = 0$, and operates *via* the symmetry of reflection, which only allows transitions between identical symmetry states, that is $\Sigma^+ \leftrightarrow \Sigma^+, \Sigma^- \leftrightarrow \Sigma^-$, and forbids the transition between symmetric and anti-symmetric states: $\Sigma^+ \not\leftrightarrow \Sigma^-$. Based on these selection rules, it can be seen that the only allowed transition for $S(^3P) + S(^3P)$ dissociation case is $1^3\Pi_u \leftarrow 1^3\Sigma_g^-$.

In the case of dissociation to the $S(^3P) + S(^1D)$ atoms, by analyzing the parity and occupation of CI orbitals for each atom at interatomic distance of 10 Å, the combined parity of atomic term is observed to be *ungerade*, and the Wigner-Witmer rules state, that there should be $2\Sigma^+, \Sigma^-, 3\Pi, 2\Delta, \Phi$ states. In our case, the higher energy Δ, Φ states, and one Π state were not computed. Based

Table 1
$^3\Pi$ state electronic configuration and parity.

State	Configuration	Spin	Squared CI coefficient
$1^3\Pi_x$	$11_g^2 12_u^2 13_g^2 14_g^1 15_u^2 16_g^1 17_u^2 18_u^0$	↑↑	0.81
$2^3\Pi_x$	$11_g^2 12_u^2 13_g^1 14_g^0 15_u^2 16_g^1 17_u^2 18_u^2$	↑↑	0.85
$3^3\Pi_x$	$11_g^2 12_u^2 13_g^2 14_g^1 15_u^2 16_g^1 17_u^1 18_u^1$	↑↓↑↑	0.18
		↑↑↓↑	0.36
	$11_g^2 12_u^2 13_g^2 14_g^1 15_u^1 16_g^2 17_u^2 18_u^0$	↑↑	0.30
$4^3\Pi_x$	$11_g^2 12_u^2 13_g^2 14_g^1 15_u^2 16_g^1 17_u^1 18_u^1$	↑↓↑↑	0.53
		↑↑↓↑	0.22
		↑↑↑↓	0.10
$1^3\Pi_y$	$11_g^2 12_u^2 13_g^2 14_g^1 15_u^2 16_g^0 17_u^2 18_u^1$	↑↑	0.81
$2^3\Pi_y$	$11_g^2 12_u^2 13_g^1 14_g^0 15_u^2 16_g^2 17_u^2 18_u^1$	↑↑	0.85
$3^3\Pi_y$	$11_g^2 12_u^2 13_g^2 14_g^1 15_u^1 16_g^1 17_u^2 18_u^1$	↑↓↑↑	0.10
		↑↑↑↓	0.44
	$11_g^2 12_u^2 13_g^2 14_g^1 15_u^2 16_g^0 17_u^1 18_u^2$	↑↑	0.30
$4^3\Pi_y$	$11_g^2 12_u^2 13_g^2 14_g^1 15_u^1 16_g^1 17_u^2 18_u^1$	↑↓↑↑	0.59
		↑↑↓↑	0.19
		↑↑↑↓	0.07